A superconducting antenna coupled microbolometer for THz applications*

A. Luukanen[†‡], R. H. Hadfield, A. J. Miller, and E. N. Grossman
National Institute of Standards and Technology, Quantum Electrical Metrology Division
325 Broadway, Boulder, CO 80305, U.S.A

ABSTRACT

In this paper we demonstrate a superconducting bolometer, coupled to a lithographic antenna. The detector is operated at 4.2 K, and has an electrical noise equivalent power (NEP) of 14 fW/Hz$^{1/2}$. We note that this sensitivity is approaching the typical background noise limit for terrestrial observations. The attractive feature of antenna coupled microbolometers is that the simple fabrication procedure allows straightforward scaling to arrays, multi-frequency capability, as well as intrinsic polarization selectivity. These features potentially enable the remote detection of chemical or biological agents by measuring differential absorption with two or more bolometers coupled to antennas designed for the intended frequencies. The noise equivalent temperature difference attainable with these detectors is around 40 mK at 0.5 THz for 1/30 s integration time and 30 % bandwidth which would enable unprecedented image quality in concealed weapons detection applications. Although the devices require cooling to cryogenic temperatures, we note that compact, closed cycle cryocoolers exist on the market which remove the need for liquid cryogens and provide user-friendly operation.

Keywords: Bolometer, superconducting, terahertz, imaging

1. Introduction

At present, the most sensitive detectors in the THz band are heterodyne receivers which have serious limitations in terms of scalability to large arrays due to system cost. As the spectral features of gases at atmospheric pressure and solids are quite broad, the spectral resolution of heterodyne receivers becomes less relevant. In submillimeter-wave imaging There is an ever growing need for large image forming arrays of direct detectors for astronomy, remote sensing and also for ground-based applications, such as security screening, medical imaging and surveillance. Up to about 200 GHz, InP HEMT based amplifiers have been used to construct arrays up to 1040 elements[1]. At higher frequencies, practical broadband detector technology scalable to large arrays does not exist. Our goal is to develop incoherent submillimeter detectors capable of reaching the photon noise limits of 300 K blackbody radiation. For a detector with a bandwidth of about 30 % around the center frequency at 500 GHz, this corresponds to a NEP of approximately 2 fW/Hz^{½}. In this paper we present the fabrication, *I-V* characteristics, and noise performance of a novel superconducting bolometer, whose electrical NEP is already close to the photon noise limit.

2. The hot-spot microbolometer operational principle

The detector is operated at a bath temperature below the critical temperature of the suspended Nb bridge (width *w*, length *l*, thickness *t*). When a sufficient voltage bias is connected across it, the bridge switches to normal state. As the bias voltage is reduced, the approximately quadratic temperature gradient in the bridge causes the ends of the bridge cool first below the T_c and turn superconducting, while the center portion remains dissipative. The submillimeter wave radiation induces alternating currents to the bridge, which dissipate to the entire length of the bridge when operated near frequencies corresponding to the energy gap, $f_{gap}=3.52\ k_B T_c/h \approx 500$ GHz for the $T_c=6.8$ K the Nb film. The DC bias current is dissipated in the normal state region only. The *I-V* curve is obtained by solving two 1-D diffusion equations[2,3,4] ,

---

† luukanen@boulder.nist.gov; (303) 497-4590; fax (303) 497-3042

‡ on leave from VTT Information Technology, Espoo, Finland

$$
\begin{aligned}
-\kappa \frac{d^2T}{dx^2} &= \frac{V^2}{\rho_n l_n^2} + \frac{P_{opt}}{wtl_n}, \quad |x| \le l_n/2 \\
-\kappa \frac{d^2T}{dx^2} &= \frac{P_{opt}}{wtl_n}, \qquad |x| > l_n/2,
\end{aligned}
\tag{1}
$$

where κ is the thermal conductivity of the bridge material, l_n is the length of the normal state hot-spot, w and t are the width and the thickness of the bridge, respectively, and ρ_n is the normal state resistivity of the metal. . The first equation in (1) corresponds to the normal state region, while the second describes the heat balance in the superconducting region which dissipates only the optical power P_{opt}. The boundary conditions are $T(\pm l/2)=T_0$, i.e. that the ends of the bridge are at bath temperature, and that the maximum temperature occurs in the middle of the bridge, $dT/dx|_{x=0}=0$. Additionally, heat flux conservation is required at the superconductor – normal metal boundary, $dT(l_n/2)/dx|_S = dT(l_n/2)/dx|_N$ These equations are solved with respect to l_n, which yields the DC resistance of the bolometer, $R=\rho_n l_n/wt$. In the limit of small optical power ($P_{opt}<<V^2/R$) a result for the $I(V)$ is

$$
I(V) = \frac{4\kappa(T_c - T_0)wt}{Vl} + \frac{Vwt}{\rho_n l} \quad . \tag{2}
$$

The electrical responsivity of the bolometer is given by $S_I=-V^{-1}L/(1+L)$ where $L=4\beta\kappa\rho(T_c-T_0)/V^2$ is the loop gain due to negative electrothermal feedback caused by the voltage bias. The factor $\beta=(R-R_s)/(R+R_s)$ corrects for the effect of the non-zero impedance R_s of the voltage source. The noise sources of the detector are those typically encountered in resistive bolometers: thermal fluctuation noise (TFN, also known as phonon noise) arising from the thermal link between the bolometer and the heat sink, Johnson noise from the normal state part, and the noise of the preamplifier. The total electrical NEP, referred to the input of the bolometer, with contributions from these sources respectively is at low frequencies given by

$$
\mathrm{NEP} = \left[4\gamma k_B T_c^2 G + \left(\frac{k_B T_c}{R} + i_{amp}^2 \right) \frac{(1+\beta)^2 V^2}{L^2} \right]^{1/2} , \tag{3}
$$

where $G=12\kappa wt/l$ is the thermal conductance to the heat sink, and γ=0.67 describes the effect of the temperature gradient in the bridge on the TFN[5]. In the optimized case, the NEP is limited by the TFN.

3. Detector fabrication

In order to utilize the bridge architecture in large arrays, a simple yet robust fabrication method is required. The detectors are fabricated on high resistivity 525 μm thick Si wafers which have ~1 μm thick Si_3N_4 grown on both sides using a LPCVD method. The patterning of the structures was carried out using electron beam lithography, although more conventional photolithography could be used as well. A bi-layer PMMA-MAA/MAA electron-beam resist exposed and developed, then the Nb metallization, incorporating the bonding pads and the antenna, is deposited to a thickness of 100 nm using electron-gun evaporation in an UHV chamber at a rate of 3 Å/s, followed by lift-off. We note that for optical tests, a separate Au layer is required for the antenna, as the Nb is too lossy at these frequencies. After lift-off, the 15 μm x 1 μm x 100 nm bridge is released from the substrate by a dry etch using a mixture of CF_4 and O_2 gases. We perform the RIE at a relatively high pressure of ~50 mTorr, which results to isotropic etching of the underlying Si_3N_4 and Si. The resulting structure is shown in Fig. 1. A large number of such supported structures have been fabricated with a yield over 90 %, implying the bolometers can readily be fabricated into an array.

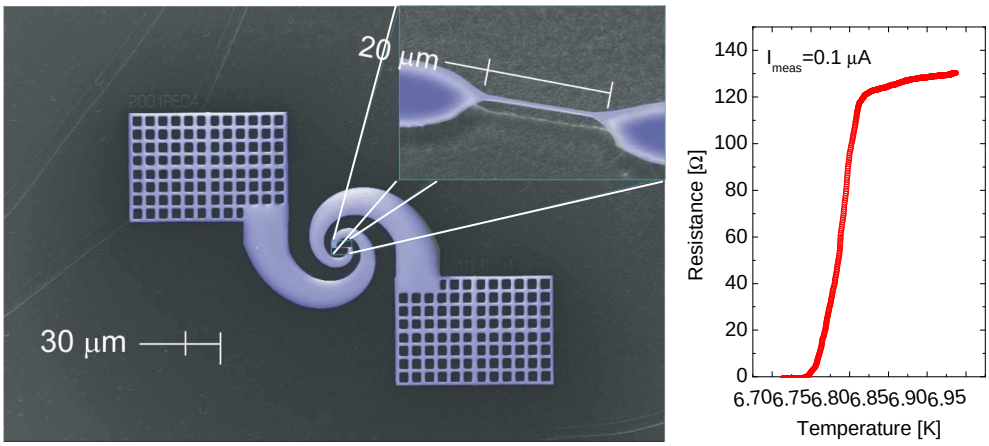

Fig. 1: (Left) A SEM image of the bolometer. The inset shows the bridge, located at the feed of the log-spiral antenna. The meshed structures are the bonding pads which connect the device to the bias circuit. (Right) The R-T curve of the bridge, measured with a small constant current bias.

4. Measurements

First, an *R-T* measurement of the bridge was performed by measuring the bridge resistance as a function of bath temperature. From this measurement, a critical temperature T_c=6.8 K and normal state resistivity ρ_n=56 $\mu\Omega$cm was obtained (using the bridge geometry described in section 3). Next, the *I*(*V*) characteristics were measured by connecting the bolometer in series with the input coil of the superconducting quantum interference device (SQUID) ammeter, while the voltage bias was provided by current biasing a 1.2 Ω resistor connected in parallel with the bolometer SQUID combination. A diagram of the bias circuit is shown in Fig. 2.

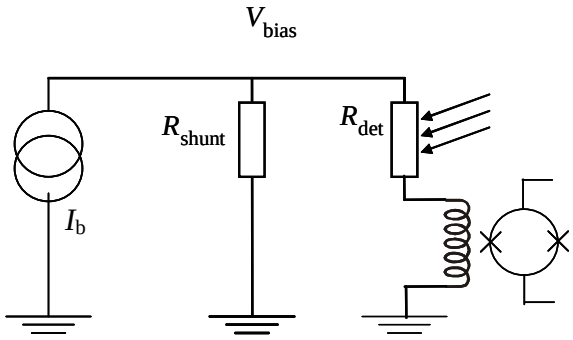

Fig. 2: The bias circuit used to measure the device *I(V)* curve and the noise spectrum.

The measured *I(V)* curve is shown in Fig. 3, together with a fit using Eq. 2. The fitting parameter was the thermal conductivity κ, for which we obtained a value 0.54 W/Km. The electrical responsivity of the bolometer was determined from the *I(V)* curve. Next, the bolometer noise was measured between 750 Hz and 25 kHz at various bias points, and the NEP was calculated using the results for the responsivity. As can be seen from the results shown in Fig.3, the electrical NEP has a minimum value of 14 fW/Hz^{½}, which is nearly an order of magnitude better than the electrical NEP of existing hot-electron bolometers operated at 4.2 K. The increase in the noise below 0.82 mV is due to instability of the bias circuit as the effective time constant of the bolometer becomes comparable to that of the bias circuit[6]. The bolometer has a remarkably large dynamic range: saturation occurs when optical power $P_{opt} \sim V^2/R$=20 nW. This yields a 30 Hz dynamic range of 54 dB.

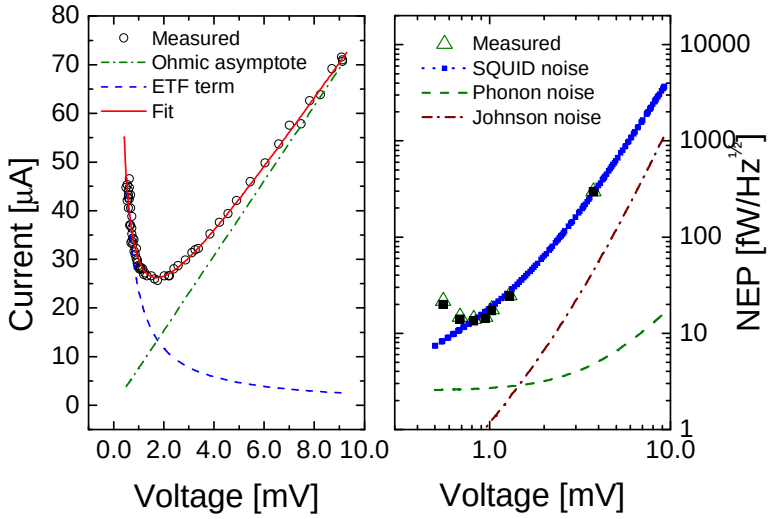

Fig. 3: (Left) The *I*(*V*) characteristics of the bolometer. (Right) The electrical NEP of the bolometer. The noise is dominated by the SQUID amplifier noise. A minimum NEP=14 fW/Hz^{½} is obtained at V=0.82 mV. With better noise matching, the phonon noise limit could be reached.

We note that better noise matching with the amplifier would enable an electrical NEP of 2.6 fW/Hz^{½,} which is already close to the photon noise limit of 2.2 fW/Hz$^{1/2}$. Here we would like to point out that as the SQUID is not particularly well noise matched (because bolometer impedance is much higher than the impedance of the SQUID), other types of amplifiers could be used as well. Direct coupling of bipolar amplifiers will degrade the noise performance, but by the use of AC bias and resonant impedance transformers the amplifier noise could be reduced significantly. With regard to the optical performance of the device, it has been shown that better than 50 % optical coupling is possible with antenna-coupled microbolometers at least up to 30 THz[7], suggesting that optical NEPs will be about twice the values quoted here.

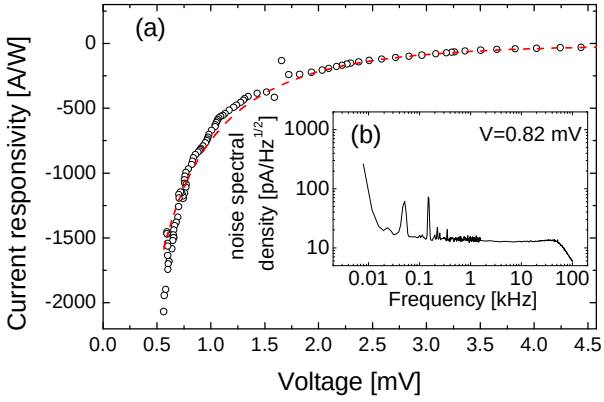

Fig. 2: a) The electrical current responsivity calculated from the *I(V)* curve (marked with circles). The dashed line is obtained from the fit to the *I(V)*. b) A noise spectrum of the device, with *V*=0.82 mV. The roll-off at ~50 kHz is due to the SQUID read-out.

A useful figure of merit for a direct detector observing blackbody sources is the noise equivalent temperature difference (NETD), given by NETD=NEP/[$\eta k_B \Delta\nu (2\tau)^{½}$] for a detector observing a single mode, with η the optical coupling efficiency, $\Delta\nu$ the pre-detection bandwidth of the sensor and τ the post-detection integration time. For realistic parameters (η=0.3, $\Delta\nu$=150 GHz, τ=30 ms), NETD=90 mK if using the electrical NEP measured for our detector and

NETD=20 mK if a detector limited NEP is reached. Both of these figures are more than adequate for many applications, such as indoors passive detection of weapons concealed under clothing. The sensitivity, combined with the large dynamic range, opens a whole range of possibilities. One particularly interesting application would be to use these devices in the remote detection of bioparticles, such as spores of anthrax[8]. In the scenario outlined in Ref. 8, a differential absorption spectroscopy method is used to identify the strong attenuation resonances of biomolecules. We note that the calculation of Ref. 8 used a detector NEP of 10^{-13} W/Hz$^{1/2}$ implying that the device described in this paper could yield substantial improvement in the detection limit in terms of range, cloud depth or spore concentration.

5. NbN bridge development

Recently, we started to investigate the possibility of using other superconducting materials for the bridge. A promising material candidate is NbN, as its higher T_c of 14 K (for thin films on Si substrates[9]) would significantly reduce the cooling power requirements for the cryocooler. Another attractive property of NbN is the fact that it has a thermal conductivity κ=0.04 – 0.08 W/Km, i.e. significantly lower than that of Nb, thus enabling further improvement in the NEP of the device. We have fabricated trial samples of NbN bridges successfully, as shown in Fig.3. The samples were fabricated by first DC magnetron sputtering of 30 nm of NbN on a Si wafer (heated to 800 °C), followed by the deposition of 150 nm of Au with the wafer at 100 °C. The wiring was defined by a photoresist mask, through which a ion mill was performed to remove the bilayer. This step was followed by a second photolithography step to define the bolometer by removing part of the top layer of Au while leaving the underlying layer of NbN intact. As a last step, a XeF_2 gas-phase chemical etch was used to selectively etch the Si substrate from under the NbN bolometer. The I(V) and noise measurements on these devices will be performed in the near future.

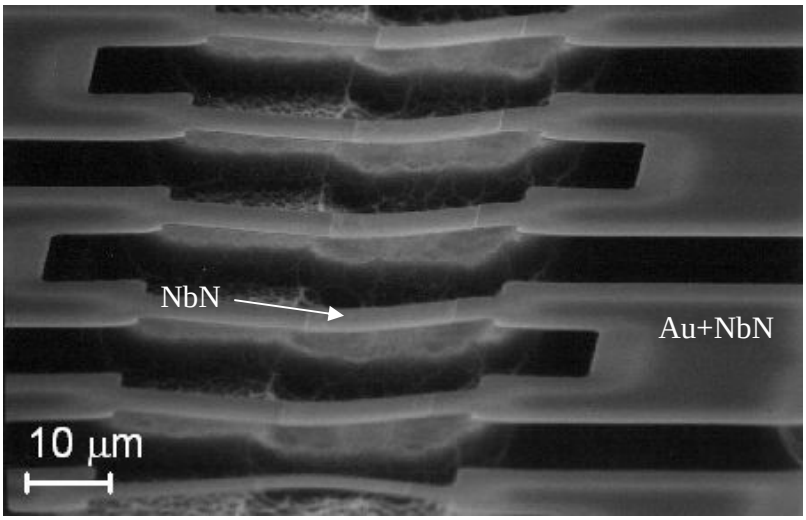

Fig. 3: A SEM image of a set of NbN vacuum-bridges.

6. Conclusions

We have demonstrated the operation of an antenna-coupled vacuum bridge bolometer, which operates in the so-called hot-spot regime. A simple fabrication process has been developed which is compatible with the construction of large arrays. Better noise matching with the preamplifier can improve the NEP to within a factor of three from the photon noise limit at (500±75) GHz. The sensitivity of the bolometer is more than sufficient for terrestrial passive

submillimeter-wave imaging from 100 GHz upwards, and could benefit a number of other applications, such as stand-off differential absorption line spectroscopy of biomolecules.

REFERENCES

[1] L. Yujiri, H. Agravante, M. Biedenbender, G. Dow, M. Flannery, S. Fornaca, B. Hauss, R. Johnson, R. Kuroda, K. Jordan, P. Lee, D. Lo, "Passive millimeter-wave camera," in Passive Millimeter-Wave Imaging Technology (R. M. Smith, ed.), vol. 3064, (Bellingham, Washington 98227-0010 USA), pp. 15–22, SPIE, SPIE, (1997).

[2] D. W. Floet, E. Miedema, and T. Klapwijk, "Hotspot mixing: A framework for heterodyne mixing in superconducting hot-electron bolometers," Appl. Phys. Lett., vol. 74, no. 3, pp. 433–435, (1999).

[3] H. F. Merkel, P. Khosropanah, S. Cherednichenko, K. Yngvesson, A. Adam, and E. L. Kollberg, "A two-dimensional hot-spot mixer model for phonon-cooled hot electron bolometers," *IEEE Trans. Appl. Supercond.*, vol. 11, pp. 179–182, (2001).

[4] A. Luukanen and J.P. Pekola, "A superconducting antenna-coupled hot-spot microbolometer", *Appl. Phys. Lett.* **82**, pp.3970-3972 (2003).

[5] J. C. Mather, "Bolometer noise: non-equilibrium theory," Appl. Opt.,vol. 21, pp. 1125–1129, March 1982.

[6] K. D. Irwin, G. C. Hilton, D. A. Wollman, and J.M. Martinis, "Thermal response time of superconducting transition-edge microcalorimeters," J. Appl. Phys., vol. 83, pp. 3978–3985, (1998).

[7] E. N. Grossman, J. E. Sauvageau, and D. G. McDonald, "Lithographic spiral antennas at short wavelengths," Appl. Phys. Lett., vol. 59, pp. 3225–3227, (1991).

[8] E.R. Brown, D.L. Woolard, A.C. Samuels, T. Globus, and B. Gelmont, "Remote detection of bioparticles in the THz region", *IEEE MTT-S*, pp. 1591-1594 (2002).

[9] N. Iossad, "Metal nitride for superconducting tunnel detectors", Ph.D. thesis, Delft University of Technology, ISBN 90-77017-96-8 (2002).